

Topological inner structures of baryons in hypersphere soliton model

Soon-Tae Hong*

Center for Quantum Spacetime and Department of Physics, Sogang University, Seoul 04107, Korea

(Dated: January 23, 2020)

Exploiting a soliton on a hypersphere we construct baryon charge density profiles possessing spherical symmetry. In this topological soliton model, we study cohomology group structure associated with a nilpotent BRST charge, and knot structure related with gluon effect and confinement problem in the quark model. We also predict baryon properties such as masses, charge radii and magnetic moments by using hypersphere Skyrmion Lagrangian with pion mass correction term.

PACS numbers: 12.39.Dc, 13.40.Em, 14.20.-c

Keywords: hypersphere Skyrmion, baryon, charge density, BRST

I. INTRODUCTION

In 1962, Dirac proposed [1] that the electron should be considered as a charged conducting surface and its shape and size should pulsate. Here the surface tension of the electron was supposed to be needed to prevent the electron from flying apart under the repulsive forces of the charge. Moreover he proposed that such an electron shape should have spherical symmetry. Motivated by this, we will consider the Skyrmion model on a hypersphere [2, 3], to study topological profile structures inside baryons.

On the other hand, the Dirac Hamiltonian scheme has been developed [4–7], to convert the second class constraints into the first class ones. Moreover, exploiting the Hamiltonian quantization method, there have been attempts to quantize the constrained systems to investigate BRST [8] symmetries involved in the systems.

In particular, the first order tetrad gravity have been investigated in the Dirac Hamiltonian scheme to see that the second class constraints reduce the theory to second order tetrad gravity and the first class constraints are different from those in the second order formalism, but satisfy the same gauge algebra if one uses Dirac brackets [5]. There have been also attempts to study the quantum BRST charge for quadratically nonlinear Lie algebras, and to derive a condition which is necessary and sufficient for the existence of a nilpotent BRST charge [6].

The standard Skyrmion model [7, 9, 10] is defined on ordinary three dimensional Euclidean space R^3 so that the mapping $U : R^3 \rightarrow S^3$ cannot fulfill homotopy group [11]. Here S^3 is the group manifold for the $SU(2)$ group structure. In the standard Skyrmion model, the three dimensional Euclidean physical space R^3 is assumed to be topologically compactified to S^3 and the spatial infinity is located on the northpole of S^3 . However in order to define strictly the homotopy group $\Pi_3(S^3) = Z$ related with the rigorous mapping $U : S^3 \rightarrow S^3$, we need the physical space S^3 , namely the hypersphere manifold, instead of R^3 which is assumed to be topologically compactified to S^3 .¹ We notice that the Skyrmion on the hypersphere has been considered [2, 3] to obtain a topological lower bound on the energy. It is also interesting to note that, in a (1+1)-dimensional supersymmetric soliton, topological boundary conditions and the BPS bound have been investigated to fix ambiguities in the quantum mass of the soliton [12].

In this paper, exploiting the hypersphere Skyrmion model, we will probe theoretically the inner structures of the baryons to investigate their charge density distributions and knot structure of a Möbius strip associated with the topological soliton. After constructing the first class Hamiltonian of the hypersphere Skyrmion, we also study the cohomology group related with the BRST charge of the geometrically constrained system.

In Sec. 2, we will study the pion mass effects on the physical properties of the baryons. In Sec. 3, we will analyze the profile and knot structures inside the nucleons. In Sec. 4, we will construct the BRST invariant Hamiltonian of the hypersphere Skyrmion to study its cohomology group structure. Sec. 5 includes conclusions.

*Electronic address: galaxy.mass@gmail.com

¹ In the standard Skyrmion model the homotopy group is not as bad as the text implies, because the homotopy group is employed as a convenient way to realize the fact that with all known soliton solution in flat space one can integrate the baryon density to yield a discrete interger [3].

II. BARYON PREDICTIONS IN HYPERSPHERE SKYRMION MODEL WITH PION MASS

We start with the Skyrminion Lagrangian of the form

$$L_S = \int d^3x \left[\frac{f_\pi^2}{4} \text{tr}(\partial_\mu U^\dagger \partial^\mu U) + \frac{1}{32e^2} \text{tr}[U^\dagger \partial_\mu U, U^\dagger \partial_\nu U]^2 + \frac{1}{2} m_\pi^2 f_\pi^2 (\text{tr } U - 2) \right], \quad (2.1)$$

where U is an $SU(2)$ chiral field, f_π is the pion decay constant, e is a dimensionless Skyrme parameter, and $m_\pi = 139 \text{ MeV}$ is the pion mass. We note that the quartic term is necessary to stabilize the soliton in the baryon sector. The last term is the pion mass term, and this term contribution is small so that we will treat it perturbatively. For the minimum soliton energy of the Skyrminion we take a hedgehog ansatz $U_0(\vec{x}) = e^{i\tau^i \hat{x}^i f(r)}$ where τ^i are Pauli matrices, $\hat{x} = \vec{x}/r$ and for unit winding number $\lim_{r \rightarrow \infty} f(r) = 0$ and $f(0) = \pi$.

Now we proceed to investigate baryon phenomenology by using the hyperspherical metric derived in Appendix A

$$ds^2(S^3) = \lambda^2 d\mu^2 + \lambda^2 \sin^2 \mu (d\theta^2 + \sin^2 \theta d\phi^2). \quad (2.2)$$

In the hypersphere Skyrminion, we obtain the soliton energy of the form

$$E = \frac{f_\pi}{e} \left[2\pi L \int_0^\pi d\mu \sin^2 \mu \left(\left(\frac{df}{d\mu} + \frac{1}{L} \frac{\sin^2 f}{\sin^2 \mu} \right)^2 + 2 \left(\frac{1}{L} \frac{df}{d\mu} + 1 \right)^2 \frac{\sin^2 f}{\sin^2 \mu} \right) + \frac{4\pi m_\pi^2 L^3}{(ef_\pi)^2} \int_0^\pi d\mu \sin^2 \mu (1 - \cos f) + 6\pi^2 \right], \quad (2.3)$$

where $L = ef_\pi \lambda$ is a radius expressed in dimensionless units. The soliton energy E has the lower bound which is the topological lower bound plus the pion mass correction. The chiral angle f in the lower bound energy satisfies equations of motion,

$$\frac{df}{d\mu} + \frac{1}{L} \frac{\sin^2 f}{\sin^2 \mu} = 0, \quad \frac{1}{L} \frac{df}{d\mu} + 1 = 0. \quad (2.4)$$

One of the simplest solutions of Eq. (2.4) is the identity map $f(\mu) = \pi - \mu$ with the condition $L = 1$.

Using the above identity map we obtain the soliton energy given by $E = \frac{f_\pi}{e} \left[3\pi^2 \left(L + \frac{1}{L} \right) + \frac{2\pi^2 m_\pi^2 L^3}{e^2 f_\pi^2} \right]$. We note that $L = ef_\pi \lambda$ is fixed to satisfy the condition $L = 1$ so that the above soliton energy can have a minimum value

$$E = \frac{f_\pi}{e} \left(6\pi^2 + \frac{2\pi^2 m_\pi^2}{e^2 f_\pi^2} \right). \quad (2.5)$$

From now on we will use the condition $L = 1$ to predict the physical properties of baryons in the hypersphere Skymion model.

In the hypersphere Skyrminion, spin and isospin states can be treated by collective coordinates

$$a^\mu = (a^0, \vec{a}), \quad (\mu = 0, 1, 2, 3), \quad (2.6)$$

corresponding to the spin and isospin collective rotation $A(t) \in SU(2)$ given by $A(t) = a^0 + i\vec{a} \cdot \vec{\tau}$. Using the chiral field $U(\vec{x}, t) = A(t)U_0(\vec{x})A^\dagger(t)$ with $U_0(\vec{x})$ being the hedgehog ansatz, we obtain the Skyrminion Lagrangian on the hypersphere

$$L_S = -E + 2\mathcal{I} \dot{a}^\mu \dot{a}^\mu, \quad (2.7)$$

where E is the soliton energy given by Eq. (2.5) and \mathcal{I} is the moment of inertia of the form

$$\mathcal{I} = \frac{3\pi^2}{e^3 f_\pi}. \quad (2.8)$$

Here we note that the moment of inertia is not affected by the pion mass correction since the pion mass Lagrangian in Eq. (2.1) does not contain derivative terms.

Performing Legendre transformation we obtain the canonical Hamiltonian

$$H = E + \frac{1}{8\mathcal{I}} \pi^\mu \pi^\mu, \quad (2.9)$$

TABLE I: The physical properties of baryons in the hypersphere Skyrmion model possessing the pion mass term, compared with experimental data. The input parameters are indicated by *.

Quantity	Prediction	Experiment	Quantity	Prediction	Experiment
$\langle r^2 \rangle_{M,I=0}^{1/2}$	0.80 fm	0.81 fm	M_N	939 MeV*	939 MeV
$\langle r^2 \rangle_{M,I=1}^{1/2}$	0.80 fm	0.80 fm	M_Δ	1132 MeV	1232 MeV
$\langle r^2 \rangle_{M,p}^{1/2}$	0.80 fm*	0.80 fm	μ_p	2.73	2.79
$\langle r^2 \rangle_{M,n}^{1/2}$	0.80 fm	0.79 fm	μ_n	-2.14	-1.91
$\langle r^2 \rangle_{E,I=0}^{1/2}$	0.76 fm	0.72 fm	$\mu_{\Delta^{++}}$	5.28	4.7 - 6.7
$\langle r^2 \rangle_{E,I=1}^{1/2}$	0.80 fm	0.88 fm	$\mu_{N\Delta}$	3.44	3.29
$\langle r^2 \rangle_p$	$(0.780 \text{ fm})^2$	$(0.805 \text{ fm})^2$	f_π	55 MeV	93 MeV
$\langle r^2 \rangle_n$	$-(0.179 \text{ fm})^2$	$-(0.361 \text{ fm})^2$	e	4.10	-

where π^μ are canonical momenta conjugate to the collective coordinates a^μ . After the canonical quantization, we arrive at the Hamiltonian

$$H = E + \frac{1}{2I}I(I+1), \quad (2.10)$$

where I ($= 1/2, 3/2, \dots$) are isospin quantum numbers. Exploiting Eq. (2.10) we find the nucleon mass M_N for $I = 1/2$ and delta hyperon mass M_Δ for $I = 3/2$, respectively

$$\begin{aligned} M_N &= ef_\pi \left(\frac{6\pi^2}{e^2} + \frac{e^2}{8\pi^2} \right) + \frac{2\pi^2 f_\pi}{e} \left(\frac{m_\pi}{ef_\pi} \right)^2, \\ M_\Delta &= ef_\pi \left(\frac{6\pi^2}{e^2} + \frac{5e^2}{8\pi^2} \right) + \frac{2\pi^2 f_\pi}{e} \left(\frac{m_\pi}{ef_\pi} \right)^2. \end{aligned} \quad (2.11)$$

Since the pion mass does not affect on the charge radii, as in the massless pion case of hypersphere Skyrmion, we have the charge radii [3]

$$\langle r^2 \rangle_{M,I=0}^{1/2} = \langle r^2 \rangle_{M,I=1}^{1/2} = \langle r^2 \rangle_{M,p}^{1/2} = \langle r^2 \rangle_{M,n}^{1/2} = \langle r^2 \rangle_{E,I=1}^{1/2} = \sqrt{\frac{5}{6}} \frac{1}{ef_\pi}, \quad (2.12)$$

$$\langle r^2 \rangle_{E,I=0}^{1/2} = \frac{\sqrt{3}}{2} \frac{1}{ef_\pi}, \quad \langle r^2 \rangle_p = \frac{19}{24} \frac{1}{(ef_\pi)^2}, \quad \langle r^2 \rangle_n = -\frac{1}{24} \frac{1}{(ef_\pi)^2}. \quad (2.13)$$

Next we obtain the magnetic moments

$$\begin{aligned} \mu_p &= \frac{2M_N}{ef_\pi} \left(\frac{e^2}{48\pi^2} + \frac{\pi^2}{2e^2} \right), & \mu_n &= \frac{2M_N}{ef_\pi} \left(\frac{e^2}{48\pi^2} - \frac{\pi^2}{2e^2} \right), \\ \mu_{\Delta^{++}} &= \frac{2M_N}{ef_\pi} \left(\frac{e^2}{16\pi^2} + \frac{9\pi^2}{10e^2} \right), & \mu_{N\Delta} &= \frac{2M_N}{ef_\pi} \cdot \frac{\sqrt{2}\pi^2}{2e^2}, \end{aligned} \quad (2.14)$$

where the nucleon mass M_N is changed due to the pion mass contribution as in Eq. (2.11).

From the charge radii in Eq. (2.12) we choose $\langle r^2 \rangle_{M,p}^{1/2} = 0.80 \text{ fm}$ as an input parameter. One can then have $ef_\pi = 225.23 \text{ MeV} = (0.876 \text{ fm})^{-1}$ and, with this fixed value of ef_π , one can proceed to calculate the other charge radii as shown in Table I. Exploiting values of $M_N = 939 \text{ MeV}$ as another input parameter, we evaluate the delta hyperon mass to yield $M_\Delta = 1132 \text{ MeV}$. The predictions for M_Δ and the other quantities are listed in Table I. We note that the predictions with the massive pion are comparable to the corresponding experimental data as shown in Table I. In particular, one can realize that the predictions for M_N , M_Δ and μ_p in the massive pion case are much more improved compared to those in the massless pion one [3].

Now we investigate the physical meaning of the radius λ of the hypersphere. Inserting the above value $ef_\pi = (0.876 \text{ fm})^{-1}$ into the condition $L = ef_\pi \lambda = 1$, we obtain the value of λ

$$\lambda = 0.876 \text{ fm}. \quad (2.15)$$

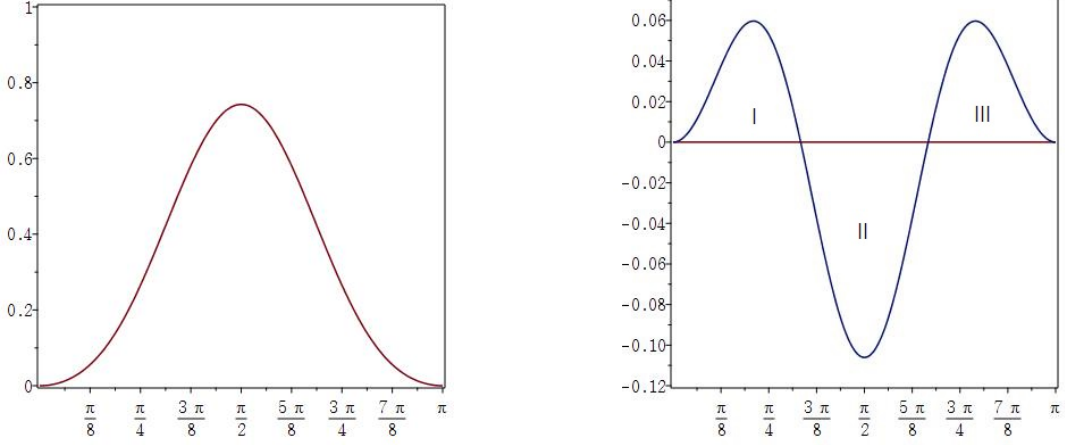


FIG. 1: The density distributions $\rho_N(\mu)$ for (a) proton and (b) neutron are plotted versus μ .

Here we emphasize that the above value is the size of hypersphere radius. To make its meaning clear, we consider one dimensional case. The radius of circle S^1 is finite but a stereographic projection maps the circle to the straight line including infinity as shown in Figure 2 below. Moreover one can readily see that the circle with any radius size contains the property of infinity since one can trace the circle infinitely many times. Next we consider two dimensional spherical shell S^2 of radius R . The shell can be made of circles S^1 with radius $R \sin \theta$ where θ is the angle defining the position of S^1 . Here we note that all the radii of the circles are less than the radius of the spherical shell of radius R . Similarly, in the three dimensional hypersphere of radius λ , all the spherical shell radii $\lambda \sin \mu$ are also less than the radius λ of the hypersphere as shown in Figure 7 in Appendix A. The hypersphere is made of two dimensional spherical shell S^2 and one dimensional circle S^1 of radius λ . Moreover the maximum value of the radius of the spherical shell is λ . The hypersphere Skymion is thus defined inside the radius λ whose value is given in Eq. (2.15). This radius value $\lambda = 0.876$ fm is comparable to the predictions for the charge radii in Eq. (2.12) given in Table I. Moreover the relations in Eq. (2.12) strongly support that the baryon phenomenology is well described in terms of the Skymion defined on S^3 embedded in Euclidean physical space R^4 .

III. TOPOLOGICAL INTERNAL STRUCTURES OF NUCLEONS

Now we investigate charge density profiles, knot structure, gluon effect and confinement problem. Using the hypersphere metric in Eq. (2.2), we construct the proton and neutron charge densities of the form

$$\rho_p(\mu) = \frac{1}{\pi} \sin^2 \mu \left(1 + \frac{4}{3} \sin^2 \mu \right), \quad \rho_n(\mu) = \frac{1}{\pi} \sin^2 \mu \left(1 - \frac{4}{3} \sin^2 \mu \right). \quad (3.1)$$

We then find the proton and neutron charges as follows

$$Q_p = \int_0^\pi d\mu \rho_p(\mu), \quad Q_n = \int_0^\pi d\mu \rho_n(\mu), \quad (3.2)$$

which yield

$$Q_p = 1, \quad Q_n = 0, \quad (3.3)$$

as expected.

The proton and neutron charge densities in Eq. (3.1) are depicted in Figure 1 (a) and Figure 1 (b), respectively. From Eq. (3.1) we find two root values of $\rho_n(\mu)=0$: $\mu = \frac{\pi}{3}$ and $\mu = \frac{2\pi}{3}$. We now have three regions I, II and III in the neutron charge density as shown in Figure 1 (b) and for each region, we obtain the charge fractions as follows

$$Q_n^I = \frac{\sqrt{3}}{16\pi}, \quad Q_n^{II} = -\frac{\sqrt{3}}{8\pi}, \quad Q_n^{III} = \frac{\sqrt{3}}{16\pi}, \quad (3.4)$$

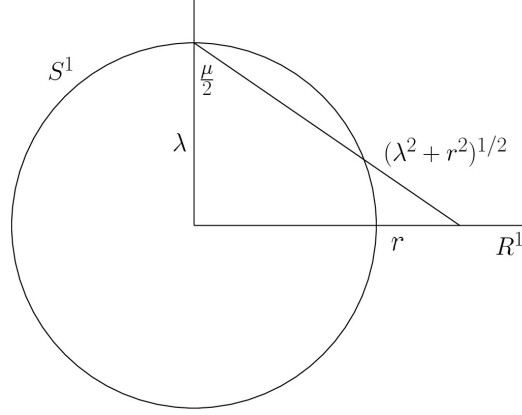


FIG. 2: The stereographic projection from S^1 to R^1 is defined in terms of μ , r and λ .

which are in good agreement with the result $Q_n = 0$. Here we note that the charge density distribution of neutron has no dependence on the coordinates θ and ϕ and it has dependence only on the coordinate μ , radial distance analogue defined on S^1 . The charge density distributions of the neutron and proton in the hypersphere Skyrmon model are thus (hyper)spherically symmetric, similar to the mass density distribution inside the Earth. This feature is contradictory to the quark model, where the charge density distributions are localized on three points without spherical symmetry inside the nucleons. Moreover, in the neutron the charge density distribution curve is not flat with zero value. This means that the neutron has nontrivial charge density distribution along the radial direction. Here we emphasize that the spherical symmetry of the charge density distributions of the nucleons is similar to that of the electron proposed by Dirac [1].

Next we investigate the stereographic projection which relates $S^3 = S^2 \times S^1$ geometry to $R^3 = S^2 \times R^1$ one in the hypersphere Skyrmon. To do this, we define the stereographic projection in terms of the third angle μ and the hypersphere radius λ

$$\cos \frac{\mu}{2} = \frac{\lambda}{(\lambda^2 + r^2)^{1/2}}, \quad \sin \frac{\mu}{2} = \frac{r}{(\lambda^2 + r^2)^{1/2}}. \quad (3.5)$$

Here one notes that the northpole located at the third angle $\mu = \pi$ corresponds to the spatial infinity which is not contained in R^3 . The stereographic projection from S^1 to R^1 is depicted in Figure 2.

Using Eq. (3.5) we obtain the chiral angle in the identity map $f(\mu) = \pi - \mu$ in terms of r and λ ,

$$f(r) = \pi - \cos^{-1} \frac{\lambda^2 - r^2}{\lambda^2 + r^2}. \quad (3.6)$$

Here one notes that $f(r)$ in Eq. (3.6) is different from the chiral angle in the standard Skyrmon model since $f(r)$ is obtained through the stereographic projection (3.5) using the chiral angle $f(\mu)$ defined on S^3 hypersphere. The chiral angle $f(r)$ in Eq. (3.6) is depicted in Figure 3.

Now exploiting the stereographic projection we obtain the proton and neutron charge densities in terms of r and λ ,

$$\begin{aligned} \rho_p(r) &= \frac{1}{\pi} \frac{2\lambda}{\lambda^2 + r^2} \left(\frac{2\lambda r}{\lambda^2 + r^2} \right)^2 \left[1 + \frac{4}{3} \left(\frac{2\lambda r}{\lambda^2 + r^2} \right)^2 \right], \\ \rho_n(r) &= \frac{1}{\pi} \frac{2\lambda}{\lambda^2 + r^2} \left(\frac{2\lambda r}{\lambda^2 + r^2} \right)^2 \left[1 - \frac{4}{3} \left(\frac{2\lambda r}{\lambda^2 + r^2} \right)^2 \right], \end{aligned} \quad (3.7)$$

which are depicted in Figure 4 (a) and Figure 4 (b), respectively. Similar to the above results mentioned about $\rho_n(\mu) = 0$, we obtain two root values of $\rho_n(r)=0$: $r = \frac{\lambda}{\sqrt{3}}$ and $r = \sqrt{3}\lambda$. Exploiting the nucleon charge densities in Eq. (3.7), we obtain $Q_p = \int_0^\infty dr \rho_p(r)$ and $Q_n = \int_0^\infty dr \rho_n(r)$ which reproduce $Q_p = 1$ and $Q_n = 0$ as in Eq. (3.3).

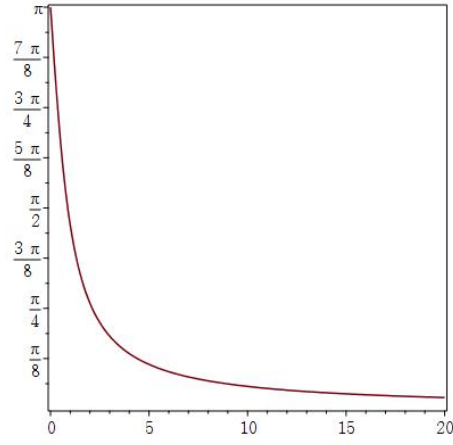


FIG. 3: The chiral angle $f(r)$ is plotted versus radial distance r in unit of fm.

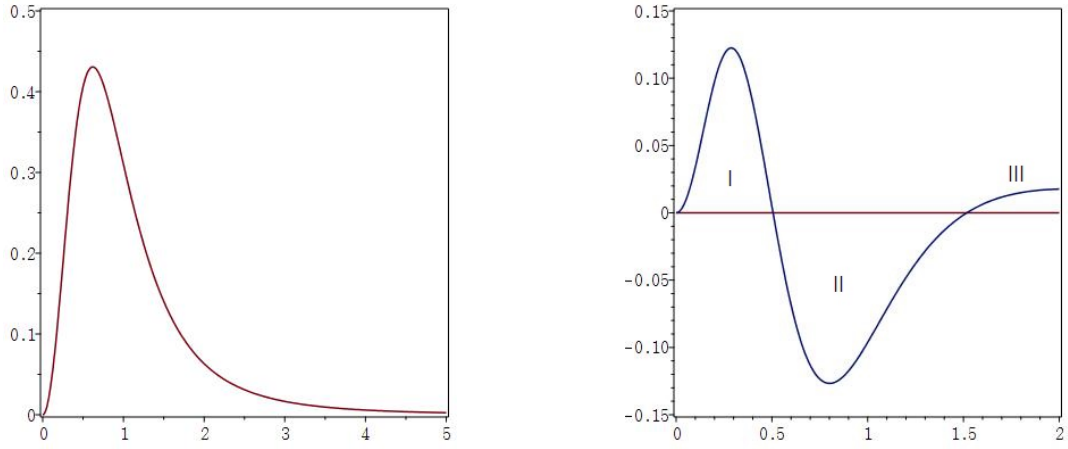


FIG. 4: The charge density distribution $\rho_N(r)$ for (a) proton and (b) neutron are plotted versus radial distance r in unit of fm.



FIG. 5: The (a) ordinary and (b) Möbius strips correspond to the boson and fermion, respectively.



FIG. 6: The Möbius strip with knot structure explains the gluon effect and confinement problem.

Moreover, we have again three regions I, II and III in the neutron charge density as shown in Figure 4 (b). For each region, we obtain consistently the charge fractions in Eq. (3.4), as expected.

Now we investigate the topological structure of Skyrmion on the hypersphere S^3 . To this, we exploit the simplified compact manifold S^1 instead of S^3 . In soliton physics in one dimension, it is well known that an ordinary strip shown in Figure 5 (a) represents a boson. However, to describe a fermion, we need a Möbius strip possessing writhing number one as shown in Figure 5 (b). To relate the hypersphere Skyrmion model to the quark model where, in the fermion such as proton and neutron, there exist three quarks, we separate the Möbius strip into three pieces as shown in Figure 5 (b) to yield two Möbius strips which are linked to each other, as shown in Figure 6. More specifically, we have the Möbius strip with the circumference length equal to that of the original Möbius strip in Figure 5 (b) and with writhing number one. This small Möbius strip originates from the middle piece of the Möbius strip in Figure 5 (b). Next we have the other Möbius strip with the circumference length of two times that of the original Möbius strip in Figure 5 (b) and with writhing number two. This large Möbius consists of the first and third pieces of the Möbius strip in Figure 5 (b). Here the writhing number two originates from addition of those of the first and third pieces of the original Möbius strip. Moreover the large strip corresponds to uu in uud and dd in udd for proton and neutron defined in quark based model, respectively.

We emphasize that two Möbius strips are linked to produce a knot structure. Due to this knot structure, the soliton is unbroken to yield the strong interaction feature. In other words, the gluon effects in the quark model can be explained by the knot structure of the Möbius strips in the hypersphere Skyrmion model. The confinement problem associated with the gluon effects among quarks has been described in terms of asymptotic freedom in the theory of the strong interaction [13]. We emphasize again that the confinement problem can be explained by the knot structure of the Möbius strips associated with the topological soliton which delineates the inner structures of the baryons.

Next we can classify the boson and fermion in terms of the strip structures. The boson performs 2π rotation to return its starting situation. This feature can be explained by exploiting 2π rotation on the ordinary strip shown in Figure 5 (a). Next the fermion performs 4π rotation to return its initial situation according to the relativistic quantum mechanics. This feature can be explained by using 4π rotation on the Möbius strip shown in Figure 5 (b). The baryonic inner structure is thus successfully explained on the S^3 hypersphere manifold embedded in the R^4 Euclidean space. This statement is one of main themes of our result. In contrast, in the case of bosonic inner structure, we do not need to consider such a hypersphere geometry.

IV. COHOMOLOGY

In this section, we investigate the cohomology involved in the hypersphere Skyrmion model. Before we get started on the cohomology in the hypersphere Skyrmion model, we briefly introduce the de Rham cohomology in algebraic topology [7, 14–16]. In this formalism we consider a d operator, namely exterior differentiation

$$d : \omega_p \rightarrow \omega_{p+1}, \quad (4.1)$$

where ω_p is a p -form. The d operator then satisfies, for all forms ω_p ,

$$d^2 \omega_p = 0. \quad (4.2)$$

In R^3 , d acts like the gradient on 0-forms, the curl on 1-forms and the divergence on 2-forms. We thus have the identity $d^2 = 0$ in Eq. (4.2) as follows

$$\nabla \times (\nabla f) = 0, \quad \nabla \cdot (\nabla \times \vec{v}) = 0, \quad (4.3)$$

for any scalar function f and vector \vec{v} [15]. A p -form ω_p is defined to be closed if $d\omega_p = 0$, while it is defined to be exact if $\omega_p = d\omega_{p-1}$ for some form ω_{p-1} . Exploiting the property (4.2), one readily checks that, for a given exact form $\omega_p (= d\omega_{p-1})$, $d\omega_p = d^2\omega_{p-1} = 0$, which means that every exact form is closed.

By using the d operator in Eq. (4.1), we define p -th de Rham cohomology group $C^p(M, R)$ of the manifold M and the field of real number R with the following quotient group [7, 14–16]

$$C^p(M, R) = \frac{Z^p(M, R)}{B^p(M, R)}, \quad (4.4)$$

where $Z^p(M, R)$ are the collection of all d -closed p -forms ω_p for which $d\omega_p = 0$, and $B^p(M, R)$ are the collection of all d -exact p -forms ω_p for which $\omega_p = d\omega_{p-1}$. Moreover the d -closed p -form ω_p is deformed into the other d -closed p -form $\omega'_p = \omega_p + d\omega_{p-1}$. Namely ω_p is homologous to ω'_p under the d operator: $\omega_p \sim \omega'_p$, since $d\omega_{p-1} = \omega'_p - \omega_p$.

Next we consider the first class Dirac formalism. In the hypersphere Skyrmion, we have the second class constraints $\Omega_1 = a^\mu a^\mu - 1 \approx 0$ and $\Omega_2 = a^\mu \pi^\mu \approx 0$, so that we have the Poisson algebra $\Delta_{kk'} = \{\Omega_k, \Omega_{k'}\} = 2\epsilon^{kk'} a^\mu a^\mu$. The hypersphere Skyrmion model thus becomes a second class constrained Hamiltonian system. Following the Dirac Hamiltonian quantization procedure, we find the first class constraints $\tilde{\Omega}_i$ ($i = 1, 2$)

$$\tilde{\Omega}_1 = a^\mu a^\mu - 1 + 2\theta = 0, \quad \tilde{\Omega}_2 = a^\mu \pi^\mu - a^\mu a^\mu \pi_\theta = 0, \quad (4.5)$$

where (θ, π_θ) are the Stückelberg fields. The first class constraints now satisfy $\{\tilde{\Omega}_1, \tilde{\Omega}_2\} = 0$. The first class physical fields \tilde{a}^μ and $\tilde{\pi}^\mu$ are given in terms of the original physical fields a^μ and π^μ , and the Stückelberg fields θ and π_θ as follows [7]

$$\begin{aligned} \tilde{a}^\mu &= a^\mu \left[1 - \sum_{n=1}^{\infty} \frac{(-1)^n (2n-3)!!}{n!} \frac{\theta^n}{a^\nu a^\nu} \right] = a^\mu \left(\frac{a^\nu a^\nu + 2\theta}{a^\nu a^\nu} \right)^{1/2}, \\ \tilde{\pi}^\mu &= (\pi^\mu - a^\mu \pi_\theta) \left[1 + \sum_{n=1}^{\infty} \frac{(-1)^n (2n-1)!!}{n!} \frac{\theta^n}{a^\nu a^\nu} \right] = (\pi^\mu - a^\mu \pi_\theta) \left(\frac{a^\nu a^\nu}{a^\nu a^\nu + 2\theta} \right)^{1/2}, \end{aligned} \quad (4.6)$$

which fulfill $\{\tilde{\Omega}_i, \tilde{a}^\mu\} = 0$ and $\{\tilde{\Omega}_i, \tilde{\pi}^\mu\} = 0$. We next obtain the first class Hamiltonian of the form

$$\tilde{H} = E + \frac{1}{8\mathcal{I}} (\pi^\mu - a^\mu \pi_\theta) (\pi^\mu - a^\mu \pi_\theta) \frac{a^\nu a^\nu}{a^\nu a^\nu + 2\theta}. \quad (4.7)$$

Here we note that the first class Hamiltonian is strongly involutive with the first class constraints $\{\tilde{\Omega}_i, \tilde{H}\} = 0$.

Now, in order to obtain the BRST invariant gauge fixed Lagrangian, we introduce two canonical sets of ghost and anti-ghost fields $(\mathcal{C}^i, \bar{\mathcal{P}}_i)$ and $(\mathcal{P}^i, \bar{\mathcal{C}}_i)$ ($i = 1, 2$) together with Stückelberg fields $(\mathcal{N}^i, \mathcal{B}_i)$ ($i = 1, 2$). Here \mathcal{C}^i and \mathcal{P}^i are ghost number $(+1)$ -forms while $\bar{\mathcal{C}}_i$ and $\bar{\mathcal{P}}_i$ are ghost number (-1) -forms. The ghost and anti-ghost and Stückelberg fields satisfy the super-Poisson algebra $\{\mathcal{C}^i, \bar{\mathcal{P}}_j\} = \{\mathcal{P}^i, \bar{\mathcal{C}}_j\} = \{\mathcal{N}^i, \mathcal{B}_j\} = \delta_j^i$.

Next we define the BRST charge

$$Q = \mathcal{C}^i \tilde{\Omega}_i + \mathcal{P}^i \mathcal{B}_i, \quad (4.8)$$

with which we define δ operator as follows

$$\delta \cdot = \{Q, \cdot\}. \quad (4.9)$$

Explicitly Q is the generator of the following infinitesimal BRST transformations

$$\begin{aligned} \delta a^\mu &= -\mathcal{C}^2 a^\mu, & \delta \pi^\mu &= 2\mathcal{C}^1 a^\mu + \mathcal{C}^2 (\pi^\mu - 2a^\mu \pi_\theta), \\ \delta \theta &= \mathcal{C}^2 a^\mu a^\mu, & \delta \pi_\theta &= 2\mathcal{C}^1, \\ \delta \mathcal{C}^i &= 0, & \delta \bar{\mathcal{P}}_i &= \tilde{\Omega}_i, \\ \delta \mathcal{P}^i &= 0, & \delta \bar{\mathcal{C}}_i &= \mathcal{B}_i, \\ \delta \mathcal{N}^i &= -\mathcal{P}^i, & \delta \mathcal{B}_i &= 0. \end{aligned} \quad (4.10)$$

Moreover we find for all the above fields

$$\delta^2 \cdot = \{Q, \{Q, \cdot\}\} = 0, \quad (4.11)$$

which is related with the nilpotent BRST charge Q .

Now we define the fermionic gauge fixing function Ψ

$$\Psi = \bar{C}_i \chi^i + \bar{\mathcal{P}}_i \mathcal{N}^i. \quad (4.12)$$

Choosing the unitary gauge: $\chi^1 = \Omega_1$ and $\chi^2 = \Omega_2$, we have $\{Q, \{Q, \Psi\}\} = 0$, which implies

$$\delta^2 \Psi = \delta\{Q, \Psi\} = 0. \quad (4.13)$$

The gauge fixed BRST invariant Hamiltonian is then given by

$$H_{eff} = \tilde{H}' - \{Q, \Psi\}, \quad (4.14)$$

where

$$\tilde{H}' = \tilde{H} + \frac{1}{4\mathcal{I}} \pi_\theta \tilde{\Omega}_2 - \frac{1}{2\mathcal{I}} \mathcal{C}^1 \bar{\mathcal{P}}_2. \quad (4.15)$$

Here \tilde{H} is given by Eq. (4.7) and the last term is Faddeev-Popov ghost term associated with the ghost and anti-ghost fields, \mathcal{C}^1 and $\bar{\mathcal{P}}_2$, respectively.

Next we exploit the BRST operator δ in Eq. (4.9) to define the cohomology associated with Q

$$\delta : \alpha_p \rightarrow \alpha_{p+1}, \quad (4.16)$$

where α_p is a ghost number p -form. We then can construct the p -th de Rham type cohomology group $C^p(M, R)$ of the manifold M and the field of real number R with the quotient group $C^p(M, R) = \frac{Z^p(M, R)}{B^p(M, R)}$. We note that this cohomology group is similar to the de Rham one in Eq. (4.4), and $Z^p(M, R)$ are now the collection of all Q -closed ghost number p -forms α_p for which $\delta\alpha_p = 0$, and $B^p(M, R)$ are the collection of all Q -exact ghost number p -forms α_p for which $\alpha_p = \delta\alpha_{p-1}$. Next, in terms of the cohomology, the Hamiltonians \tilde{H}' and H_{eff} are readily shown to be the ghost number 0-forms, and they are Q -closed

$$\delta\tilde{H}' = \{Q, \tilde{H}'\} = 0, \quad \delta H_{eff} = \{Q, H_{eff}\} = 0, \quad (4.17)$$

where we have used the identities in Eq. (4.10).

Moreover we notice that Ψ is the ghost number (-1) -form and $\{Q, \Psi\}$ is Q -exact ghost number 0-form since $\{Q, \Psi\}$ can be rewritten as $\delta\Psi$, which satisfies the identity in Eq. (4.13). Here one notes that in order to guarantee the BRST invariance of H_{eff} we have included in H_{eff} the Q -exact term $\{Q, \Psi\}$, and in \tilde{H}' the term possessing π_θ and the Faddeev-Popov ghost term. Moreover the term $\{Q, \Psi\}$ fixes the particular unitary gauge corresponding to the fixed point $(\theta = 0, \pi_\theta = 0)$ in the gauge degrees of freedom associated with two dimensional internal phase space coordinates (θ, π_θ) , which are two canonically conjugate Stückelberg fields.

Now the Hamiltonians \tilde{H}' and H_{eff} thus can be used to define $Z^0(M, R)$. Here M is the non-compact Hilbert space of the hypersphere Skyrmion model and R is the real number field. The $\{Q, \Psi\}$ can be used to define the $B^0(M, R)$. With these $Z^0(M, R)$ and $B^0(M, R)$, we construct the 0-th de Rham type cohomology group $C^0(M, R)$ for the hypersphere Skyrmion model

$$C^0(M, R) = \frac{Z^0(M, R)}{B^0(M, R)}. \quad (4.18)$$

It is interesting to note that the ghost number 0-form H_{eff} is deformed into the other ghost number 0-form \tilde{H}' . Namely H_{eff} is homologous to \tilde{H}' under the BRST transformation δ associated with Q ,

$$H_{eff} \sim \tilde{H}', \quad (4.19)$$

since $\{Q, \Psi\} = \tilde{H}' - H_{eff}$.

V. CONCLUSIONS

In summary, we have evaluated the physical properties, such as masses, charge radii and magnetic moments, of the baryons, and also have obtained their charge density profiles possessing spherical symmetry. To do this we have used the hypersphere Skyrmion with pion mass correction term. In this model, we have constructed the first class Hamiltonian to study the cohomology group structure associated with the nilpotent BRST charge.

In particular, we have noticed that the pion mass effects on the physical properties of the baryons improve their predictions so that these predicted values are quite in good agreement with their corresponding experimental data. The interesting feature of the hypersphere Skyrmion is that the baryons are delineated in terms of the knot structure of the Möbius strips. The knot can thus explain the corresponding gluon effect and confinement problem in the quark related model such as quantum chromodynamics.

It seems appropriate to comment on the quark-gluon plasma state in the quark model. This state means that the knot structure is broken up in the hypersphere Skyrmion model. The Alice detector of the Large Hadron Collider is scheduled to detect the quark-gluon plasma state, which is assumed to exist in an extremely hot soup of massive quarks and massless gluons. The quark-gluon plasma state is supposed to occur immediately after the Big Bang of the tiny early universe manufactured in the Large Hadron Collider. In the standard cosmology, the quark-gluon plasma state can exist shortly and disappear eventually to enter the radiation dominated phase. It is expected that the Alice will be able to detect the procedure of particle states along with the evolution of the tiny universe planned to occur at the Large Hadron Collider. We recall that as far as radiation and matter are concerned, the mixture of these two exists together in the current universe.

Acknowledgments

The author was supported by Basic Science Research Program through the National Research Foundation of Korea funded by the Ministry of Education, NRF-2019R1I1A1A01058449. He would like to thank Peter van Nieuwenhuizen for helpful correspondence and kind encouragement.

Appendix A: Hypersphere geometry

Before we investigate the S^3 hypersphere geometry, we briefly recapitulate the spherical coordinates by introducing the coordinates (x, y, z) in R^3

$$x = r \sin \theta \cos \phi, \quad y = r \sin \theta \sin \phi, \quad z = r \cos \theta. \quad (\text{A.1})$$

Here r is the radius of S^2 which is described in terms of the spherical shell coordinates (θ, ϕ) . The coordinates (x, y, z) thus satisfy S^2 spherical shell condition

$$x^2 + y^2 + z^2 = r^2, \quad (\text{A.2})$$

which shows that S^2 spherical shell with radius r is embedded in three dimensional Euclidean space R^3 . The ranges of the spherical coordinates are given by $0 \leq r < \infty$, $0 \leq \theta \leq \pi$ and $0 \leq \phi \leq 2\pi$.

In R^3 , the three metric is given by

$$ds^2(R^3) = dx^2 + dy^2 + dz^2 = dr^2 + r^2 (d\theta^2 + \sin^2 \theta d\phi^2). \quad (\text{A.3})$$

The line element is given by

$$d\vec{x} = \hat{e}_r dr + \hat{e}_\theta r d\theta + \hat{e}_\phi r \sin \theta d\phi, \quad (\text{A.4})$$

where $(\hat{e}_r, \hat{e}_\theta, \hat{e}_\phi)$ are the unit vectors along the three directions. Similarly, the area elements are given by

$$d\vec{a}_r = \hat{e}_r r^2 \sin \theta d\theta d\phi, \quad d\vec{a}_\theta = \hat{e}_\theta r \sin \theta dr d\phi, \quad d\vec{a}_\phi = \hat{e}_\phi r dr d\theta, \quad (\text{A.5})$$

and the volume element is defined as

$$d^3x = r^2 \sin \theta dr d\theta d\phi. \quad (\text{A.6})$$

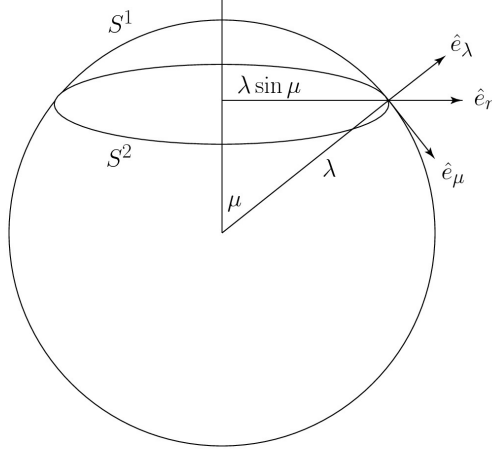


FIG. 7: The S^3 geometry is depicted in terms of $S^2 \times S^1$. Here S^2 is simplified by S^1 , for convenience.

In the spherical coordinates system, the gradient operator is given by

$$\nabla = \hat{e}_r \frac{\partial}{\partial r} + \hat{e}_\theta \frac{1}{r} \frac{\partial}{\partial \theta} + \hat{e}_\phi \frac{1}{r \sin \theta} \frac{\partial}{\partial \phi}. \quad (\text{A.7})$$

Next we consider an S^3 hypersphere embedded in R^4

$$R^3 \subset S^3 (= R^3 + \{\infty\}) \subset R^4. \quad (\text{A.8})$$

Here one notes that even though S^3 is embedded in a four dimensional manifold R^4 , S^3 itself is a three dimensional manifold. This statement can be readily understood if we consider two dimensional situation. Namely a spherical shell S^2 is a two dimensional manifold even though it is embedded in three dimensional manifold R^3 . Moreover the reason why S^2 needs three dimensional embedding manifold R^3 is that S^2 is defined as follows

$$R^2 \subset S^2 (= R^2 + \{\infty\}) \subset R^3. \quad (\text{A.9})$$

In order to investigate the Skyrmion on the hypersphere of radius λ , we introduce the coordinates (x, y, z, w) in R^4 to describe a point on S^3

$$x = \lambda \sin \mu \sin \theta \cos \phi, \quad y = \lambda \sin \mu \sin \theta \sin \phi, \quad z = \lambda \sin \mu \cos \theta, \quad w = \lambda \cos \mu, \quad (\text{A.10})$$

The ranges of the hyperspherical coordinates are given by $0 \leq \mu \leq \pi$, $0 \leq \theta \leq \pi$ and $0 \leq \phi \leq 2\pi$, and λ is the radius of S^3 which is described in terms of the hypersphere coordinates (μ, θ, ϕ) .

Now we note that the coordinates (x, y, z, w) satisfy the S^3 hypersphere condition

$$x^2 + y^2 + z^2 + w^2 = \lambda^2, \quad (\text{A.11})$$

which shows that the S^3 hypersphere of radius λ is embedded in the four dimensional Euclidean space R^4 . The three metric on S^3 in R^4 is given by

$$ds^2(S^3) = dx^2 + dy^2 + dz^2 + dw^2 = \lambda^2 d\mu^2 + \lambda^2 \sin^2 \mu (d\theta^2 + \sin^2 \theta d\phi^2). \quad (\text{A.12})$$

The radial direction from the origin of S^3 defines the forth direction of R^4 . The coordinates of the R^4 thus consist of θ , ϕ , μ and λ . On the S^3 hypersphere, the three metric is given by the line element

$$d\vec{x} = \hat{e}_\mu \lambda d\mu + \hat{e}_\theta \lambda \sin \mu d\theta + \hat{e}_\phi \lambda \sin \mu \sin \theta d\phi, \quad (\text{A.13})$$

where $(\hat{e}_\mu, \hat{e}_\theta, \hat{e}_\phi)$ are the unit vectors along the three directions. The relation between $R^3 = S^2 \times R^1$ geometry and $S^3 = S^2 \times S^1$ one is depicted in Figure 7. Here S^2 of radius $\lambda \sin \mu$ is simplified by S^1 of radius $\lambda \sin \mu$, for convenience. Moreover the radial direction, associated with \hat{e}_r , from center of the simplified S^2 with radius $\lambda \sin \mu$ represents the radial direction of R^1 in $R^3 = S^2 \times R^1$. In this picture, S^2 spherical shell of the radius $\lambda \sin \mu$ meets S^1 of radius λ . Now we have \hat{e}_θ , \hat{e}_ϕ and \hat{e}_μ which are perpendicular to one another.

Next we find the following relation

$$\hat{e}_r = \hat{e}_\mu \cos \mu + \hat{e}_\lambda \sin \mu. \quad (\text{A.14})$$

Here we note that \hat{e}_r is defined only in $R^3 \subset R^4$, but \hat{e}_μ and \hat{e}_λ are defined in the part of R^4 on which S^2 of radius $\lambda \sin \mu$ does not reside.

The area elements are given by

$$d\vec{a}_\mu = \hat{e}_\mu \lambda^2 \sin^2 \mu \sin \theta \, d\theta \, d\phi, \quad d\vec{a}_\theta = \hat{e}_\theta \lambda^2 \sin \mu \sin \theta \, d\mu \, d\phi, \quad d\vec{a}_\phi = \hat{e}_\phi \lambda^2 \sin \mu \, d\mu \, d\theta, \quad (\text{A.15})$$

and the volume element is defined as

$$d^3x = \lambda^3 \sin^2 \mu \sin \theta \, d\mu \, d\theta \, d\phi. \quad (\text{A.16})$$

In the hyperspherical coordinates system, the gradient operator is given by

$$\nabla = \hat{e}_\mu \frac{1}{\lambda} \frac{\partial}{\partial \mu} + \hat{e}_\theta \frac{1}{\lambda \sin \mu} \frac{\partial}{\partial \theta} + \hat{e}_\phi \frac{1}{\lambda \sin \mu \sin \theta} \frac{\partial}{\partial \phi}. \quad (\text{A.17})$$

-
- [1] P.A.M. Dirac, Proc. Roy. Soc. Lond. A **268**, 57 (1962).
 - [2] N.S. Manton, P.J. Ruback, Phys. Lett. B **181**, 137 (1986).
 - [3] S.T. Hong, Phys. Lett. B **417**, 211 (1998).
 - [4] P.A.M. Dirac, *Lectures in Quantum Mechanics* (Yeshiva University Press, New York, 1964).
 - [5] L. Castellani, P. van Nieuwenhuizen, M. Pilati, Phys. Rev. D **26**, 352 (1982).
 - [6] K. Schoutens, A. Sevrin, P. van Nieuwenhuizen, Commun. Math. Phys. **124**, 87 (1989).
 - [7] S.T. Hong, *BRST Symmetry and de Rham Cohomology* (Springer, Heidelberg, 2015), and references therein.
 - [8] C. Becchi, A. Rouet, R. Stora, Phys. Lett. B **52**, 344 (1974); C. Becchi, A. Rouet and R. Stora, Ann. Phys. **98**, 287 (1976); I.V. Tyutin, Levedev preprint, LEBEDEV-75-39 (1975).
 - [9] T.H.R. Skyrme, Proc. Roy. Soc. A **260**, 127 (1961).
 - [10] G.S. Adkins, C.R. Nappi, E. Witten, Nucl. Phys. B **228**, 552 (1983).
 - [11] H. Toda, *Composition Methods in Homotopy Groups of Spheres* (Princeton University Press, Princeton, 1962).
 - [12] H. Nastase, M. Stephanov, P. van Nieuwenhuizen and A. Rebhan, Nucl. Phys. B **542**, 471 (1999), hep-th/9802074.
 - [13] D. Gross, F. Wilczek, Phys. Rev. Lett. **30**, 1343 (1973); H.D. Politzer, Phys. Rev. Lett. **30**, 1346 (1973).
 - [14] J.J. Rotman, *An Introduction to Algebraic Topology* (Springer-Verlag, Heidelberg, 1988); C.A. Weibel, *An Introduction to Homological Algebra* (Cambridge University Press, Cambridge, 1994); T. Frankel, *The Geometry of Physics* (Cambridge University Press, Cambridge, 1997).
 - [15] J. Baez, J.P. Muniain, *Gauge Fields, Knots and Gravity* (World Scientific, Singapore, 1994).
 - [16] S.T. Hong, Mod. Phys. Lett. A **25**, 2529 (2010), arXiv:0907.1580 [hep-th].